JACS
JOURNAL OF THE AMERICAN CHEMICAL SOCIETY
Article
pubs.acs.org/JACS

Screening of Pre-miRNA-155 Binding Peptides for Apoptosis Inducing Activity Using Peptide Microarrays

Jaeyoung Pai,[†] Soonsil Hyun,[‡] Ji Young Hyun,[†] Seong-Hyun Park,[†] Won-Je Kim,[§] Sung-Hun Bae,[∥] Nak-Kyoon Kim,[*,§] Jaehoon Yu,[*,‡] and Injae Shin[*,†]

[†]National Creative Research Center for Biofunctional Molecules, Department of Chemistry, Yonsei University, Seoul 03722, Korea
[‡]Department of Chemistry and Education, Seoul National University, Seoul 08826, Korea
[§]Advanced Analysis Center, Korea Institute of Science and Technology, Seoul 02792, Korea
[∥]CKD Research Institute, 315-20, Dongbaekjukjeon-daero, Giheung-gu, Yongin-si, Gyeonggi-do 17006, Korea

Supporting Information

ABSTRACT: MicroRNA-155, one of the most potent miRNAs that suppress apoptosis in human cancer, is overexpressed in numerous cancers, and it displays oncogenic activity. Peptide microarrays, constructed by immobilizing 185 peptides containing the C-terminal hydrazide onto epoxide-derivatized glass slides, were employed to evaluate peptide binding properties of pre-miRNA-155 and to identify its binding peptides. Two peptides, which were identified based on the results of peptide microarray and in vitro Dicer inhibition studies, were found to inhibit generation of mature miRNA-155 catalyzed by Dicer and to enhance expression of miRNA-155 target genes in cells. In addition, the results of cell experiments indicate that peptide inhibitors promote apoptotic cell death via a caspase-dependent pathway. Finally, observations made in NMR and molecular modeling studies suggest that a peptide inhibitor preferentially binds to the upper bulge and apical stem-loop region of pre-miRNA-155, thereby suppressing Dicer-mediated miRNA-155 processing.

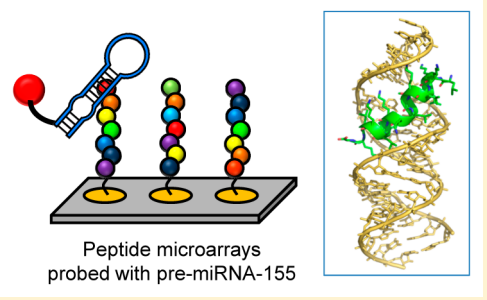

INTRODUCTION

MicroRNAs (miRNAs), short single-stranded noncoding RNAs of ca. 22 nucleotides, regulate expression of target genes through either degradation of target mRNAs or inhibition of protein translation.[1] The first step of biogenesis of miRNAs includes RNA polymerases II promoted production of primary miRNAs (pri-miRNAs).[2] The nuclear enzyme Drosha then cleaves pri-miRNAs to produce shorter stem-loop RNAs known as precursor miRNAs (pre-miRNAs).[3] After being transported into the cytosol, pre-miRNAs are processed into 21−24 base pair miRNA duplexes by Dicer.[4] One strand of the duplex becomes the mature miRNA, which functions as a gene regulator, and the other strand, termed passenger miRNA, is normally removed by degradation.[4,5] When a miRNA binds to a perfectly complementary sequence of the target mRNA, the mRNA is degraded through a similar process to the RNA interference promoted by small interfering RNAs.[6] On the other hand, binding of miRNA to the partially complementary mRNA leads to suppression of translation of target mRNAs.

It has been proposed that expressions of ca. 30% of human genes are modulated by miRNAs.[7] These RNAs play crucial roles in a wide range of physiological processes, including development, cell proliferation and differentiation, and apoptosis.[1,7] Importantly, the deregulated expression of miRNAs is associated with many pathological processes including cancer and heart disease.[8,9] Owing to their pathological significance, miRNAs have received considerable attention as targets in programs aimed at the discovery of pharmaceutical agents.

To date, several small molecules that modulate the functions of miRNAs have been developed.[10] However, despite recent progress made in the development of small molecule-based miRNA regulators, the discovery of small molecules that target miRNAs is still a highly demanded yet challenging task. The major reason for this is that the large surface area (1100−1500 A^2) of RNAs is difficult to be covered by small molecules (150 A^2).[11] Previous studies have demonstrated that peptides are potential ligands with high affinities against hairpin RNAs.[12,13] For example, we have shown that helical peptides, which strongly bind to the hairpin TAR RNA, have good inhibitory activities against TAR−Tat interactions in cells.[13,14] As a result, these peptides served as inhibitors of viral replication. The earlier findings stimulated an effort aimed at identifying peptides that regulate conversion of stem-loop pre-miRNAs to mature miRNAs by Dicer. As part of the previous effort, we observed that peptides which bind to pre-let7a-1, a tumor suppressing miRNA, promoted Dicer-catalyzed pre-let7a-1 processing, thereby enhancing cytotoxicity against cancer cells.[15] We believed that, in contrast to the role they play in enhancing Dicer activity, peptides might also disrupt Dicer-

Received: August 31, 2015
Published: January 15, 2016

DOI: 10.1021/jacs.5b09216
J. Am. Chem. Soc. 2016, 138, 857−867

mediated miRNA processing by binding to oncogenic pre-miRNAs that have stem-loop structures.

MiRNA-155, one of the most potent miRNAs that block apoptosis in human cancer,[16] is upregulated in various cancers and has oncogenic activity. Consequently, it is anticipated that peptides, which inhibit conversion of pre-miRNA-155 into mature miRNA-155 catalyzed by Dicer, would induce apoptosis of cancer cells.[17] Thus, we reasoned that peptides, which bind to the target pre-miRNA and inhibit miRNA processing, would have beneficial effects against oncogenic miRNAs.

Peptide microarrays have been widely employed for rapid analysis of protein-peptide interactions, large-scale determination of enzyme activities and high-throughput profiling of substrate specificities of enzymes.[18] Recently, we demonstrated that the peptide microarray technology also served as a robust and powerful tool for large-scale analysis of peptide-RNA interactions.[13] Owing to this feature, peptide microarrays containing 185 peptides were employed to rapidly evaluate interactions between stem-loop pre-miRNA-155 and peptides as well as to identify peptides which strongly bind to pre-miRNA-155 (Figure 1).

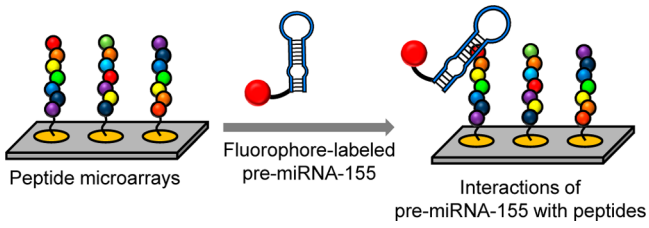

Figure 1. Peptide microarrays for studies of interactions of stem-loop pre-miRNA-155 with peptides. Peptide microarrays immobilized by various peptides are probed with fluorophore-labeled pre-miRNA-155.

As described below, two peptides, which were identified using peptide microarray assays and in vitro Dicer inhibition studies, were found to block mature miRNA-155 production from pre-miRNA-155 and to promote the expression of miRNA-155 target genes in cells. Interestingly, the peptide inhibitors induce apoptotic cell death via a caspase-dependent pathway but they do not activate AIF-associated caspase-independent apoptosis. Evidence gained from NMR and molecular modeling studies suggests that the selected peptide inhibitor interacts mainly with the upper bulge and apical stem-loop region of pre-miRNA-155, thereby blocking Dicer-catalyzed miRNA-155 processing. Observations made in the present study clearly demonstrate that peptide microarrays are powerful, high-throughput tools in studies of RNA−peptide interactions.

RESULTS AND DISCUSSION

Design and Synthesis of Peptides. Amphiphilic peptides that have helical structures are known to strongly bind to hairpin RNAs.[12] On this basis, the amphiphilic peptide LKKLLKLLKKLLKLKG (**1**), which was de novo designed to bind to calmodulin,[19] was chosen as the standard in the present study. In order to examine pre-miRNA-155 binding properties, a library containing 185 peptides was created by modifying **1** (Figure 2a and Table S1 for peptide sequence). For this purpose, the N- (peptides **2**−**5**) and C-terminal amino acids (peptides **6**−**11**) of **1** were removed one-by-one to evaluate the effect of chain length on binding to pre-miRNA-155. In addition, Lys residues in **1** were replaced by Ala (peptides **12**−**17**), which possesses a small hydrophobic side chain, and by Gln (peptides **18**−**38**), whose noncharged and hydrophilic side chain has a similar size to that of Lys. Furthermore, Leu residues in the middle region (Leu-7, 8, 11, 12) of **1** were replaced by one (peptides **39**−**42**), two (peptides **43**−**48**), three (peptides **49**−**52**), and four (peptide **53**) Gln in order to gain an understanding of the effect of hydrophobic residues on pre-miRNA-155 binding. Moreover, to determine systematically the effect of Lys and Leu in peptides on pre-miRNA-155 binding, Lys (Lys-6, 9, 10, 13) and Leu residues (Leu-7, 8, 11, 12) in the middle region of **1** were singly replaced by 18 other amino acids except cysteine (Lys-to-amino acid substitutions, **14**−**17**, **20**−**23**, **54**−**117**; Leu-to-amino acid substitutions, **39**−**42**, **118**−**185**).

A chemoselective immobilization method was employed for site-specific attachment of peptides to solid surfaces in the microarrays in order to avoid problems associated with interference from other nucleophilic side chains present in the peptides. We demonstrated earlier that peptides containing hydrazide groups were selectively and efficiently attached to epoxide-modified surfaces under mild acidic conditions (pH 5−6) even when they also contain several Lys residues.[13,20,21] To construct peptide microarrays using this immobilization technique, 185 peptides bearing C-terminal hydrazide groups were synthesized by using a standard solid-phase protocol (Figure 2b). Briefly, Wang resin was activated with *p*-nitrophenyl chloroformate and then reacted with hydrazine to give the hydrazide conjugated resin. The conjugated resin was then treated with Fmoc protected aminohexanoic acid under amide coupling conditions. After assembly of peptides on the resin, they were cleaved from the resin under acidic conditions, purified by reversed-phase HPLC, and characteized by MS analysis (Table S1).

Evaluation of Interactions between Pre-miRNA-155 and Peptides Using Peptide Microarrays. Binding properties of pre-miRNA-155 to peptides were evaluated using peptide microarrays. The microarrays were prepared by in duplicate printing 185 peptides (1 nL, 0.5 mM, pH 5.5), with the sequences described above and containing C-terminal hydrazide groups, on the epoxide-modified surface.[13,20,21] The ability of each peptide to bind pre-miRNA-155 was then determined by probing the peptide microarrays with 0.25 μM of full-length and truncated pre-miRNA-155 (U17-A50) labeled with a fluorophore at the 5′ terminus (Figure 2c). In this step, a solution of pre-miRNA-155 containing 0.05−0.5% Tween-20 was applied to peptide microarrays. The addition of Tween-20 to RNA solutions is crucial for obtaining reproducible and reliable analyses.[13] Mean values of fluorescence intensities were determined using data from five-independent experiments (<10% variation in fluorescence intensity) and scored as positive signals. The combined data set is presented as a graph of fluorescence intensities and a colored heatmap (Figure 3).

Results obtained from microarray experiments showed that both truncated and full-length pre-miRNA-155 bound to peptides with similar affinity patterns, indicating that peptides recognize the upper stem-loop region of pre-miRNA-155. Analysis of peptide microarray data also revealed that deletion and substitution of amino acids in **1** influenced binding of pre-miRNA-155 to peptides. Specifically, peptides with one to three amino acid deletions (**2**−**4**) at the N-terminus and one to four amino acid deletions (**6**-**9**) at the C-terminus of **1** interacted with RNA with gradually reduced binding affinities. However,

DOI: 10.1021/jacs.5b09216
J. Am. Chem. Soc. 2016, 138, 857−867

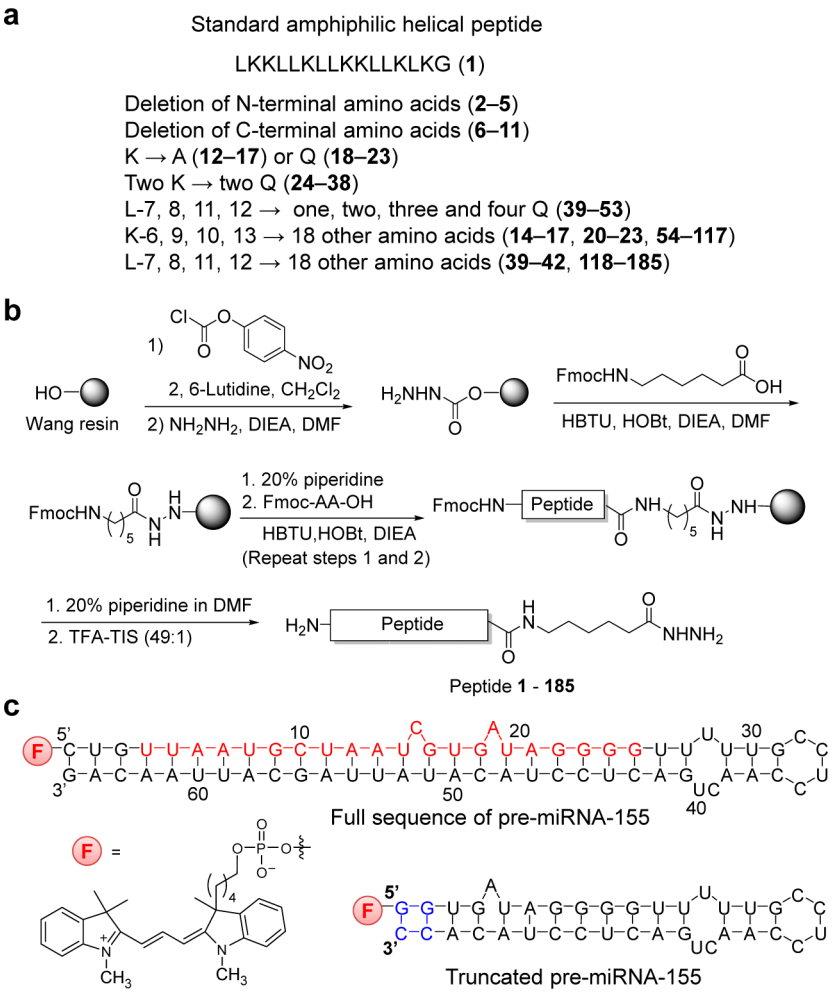

Figure 2. Sequences and synthesis of peptides and sequences of pre-miRNA-155 used in the study. (a) Peptides used for construction of peptide microarrays. (b) Synthesis of the C-terminal hydrazide-conjugated peptides (AA = amino acid). (c) Full-length and truncated pre-miRNA-155 labeled by a fluorophore (F) at the 5′-terminus (red sequence, mature miRNA-155; blue sequence, extra bases to promote formation of the stem-loop structure).

deletions of four amino acids (**5**) at the N-terminus as well as five (**10**) and six amino acids (**11**) at the C-terminus of **1** resulted in dramatically attenuated pre-miRNA-155 binding affinities. These findings suggest that amino acids 4−12 in peptide **1** are mainly involved in binding to pre-miRNA-155. Gln substitution (**18-23**) for either 6- or 10-Lys in **1** more significantly influences RNA binding than does Ala substitution at these positions. Peptides **24−38** with double Gln substitution have binding affinities to pre-miRNA-155 that depend on the position of substitution.

Analysis of the microarray data obtained from studies with peptides **39−53**, in which hydrophobic Leu residue(s) is replaced by one to four Gln, showed that peptides with more Gln substitutions interacted with pre-miRNA-155 more weakly. Peptides **43−48** with double mutations have binding affinities to pre-miRNA-155 that depend on the position of the substitution. All peptides (**49−53**) with triple and quadruple mutations bind to pre-miRNA-155 with markedly reduced affinities. These results suggest that hydrophobic Leu residues are important for binding of peptides to pre-miRNA-155.

Inspection of the microarray data arising from studies with peptides **54−117**, in which Lys is replaced by other amino acids, showed that peptides **54−101** substituted at the 6, 9, and 10 positions, respectively, recognized pre-miRNA-155 with lower binding affinities than those (**102−117**) substituted at the 13 position. In particular, substitution at the 13 position has a very little influence on pre-miRNA-155 binding. These findings suggest that Lys residues at the 6, 9, and 10 positions are critical for RNA binding but that Lys at the 13 position is involved in RNA binding to a much lesser extent. In addition, substitution of negatively charged Asp or Glu leads to attenuated pre-miRNA-155 binding affinities owing presumably to electrostatic repulsions between negatively charged residues and the phosphate groups of the RNA.[13,22]

Analysis of the microarray data obtained from studies of peptides **118−185**, in which Leu is replaced by other amino acids, revealed that peptides **118−151** substituted at 7 and 8 positions bind to pre-miRNA-155 with lower binding affinities than do those (**152−185**) substituted at 11 and 12 positions. Collectively, the results of peptide microarray experiments indicate that both the position and nature of substituted amino acid(s) influence binding of peptides to pre-miRNA-155, and that both hydrophobic and hydrophilic residues located between amino acids 4−12 of peptides are likely involved in interactions with pre-miRNA-155.

To determine the effect of peptide helicity on pre-miRNA-155 binding, circular dichroism (CD) spectra of **1** and 18 other peptides (**16**, **22**, **86−101**), mutated at the 10 position, were

DOI: 10.1021/jacs.5b09216
J. Am. Chem. Soc. 2016, 138, 857−867

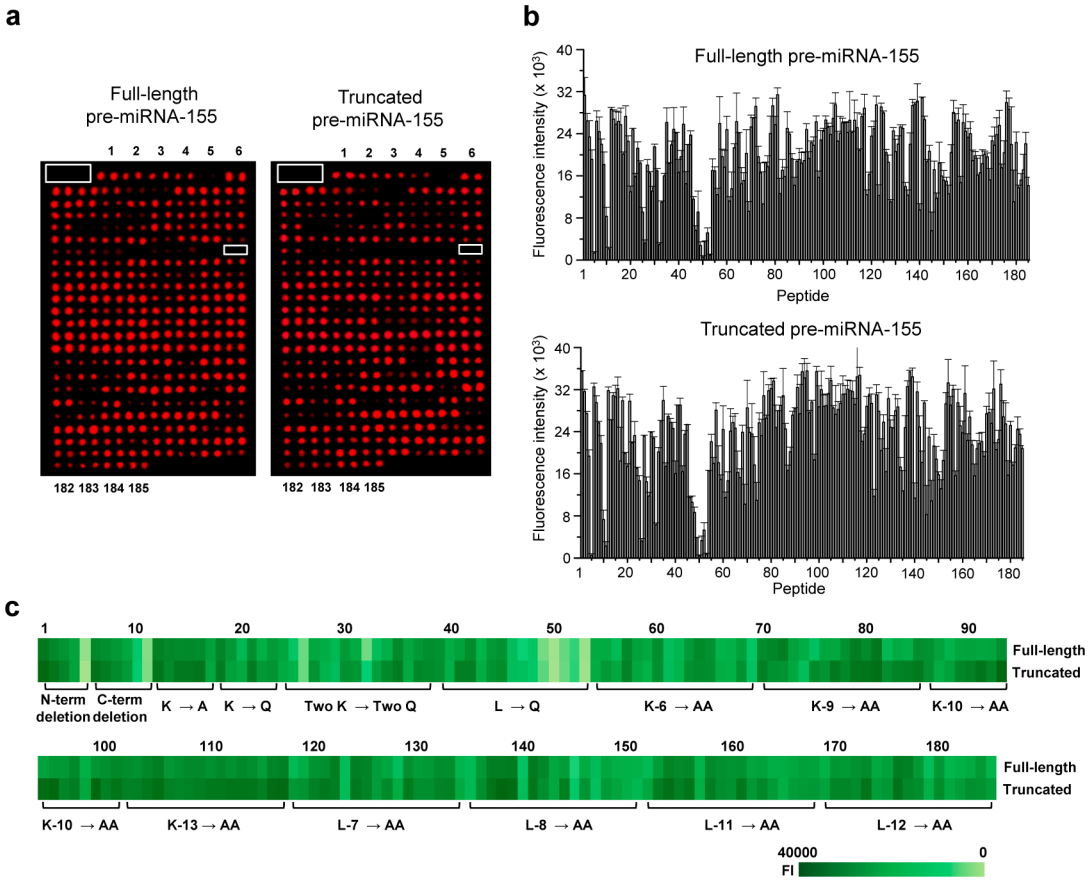

Figure 3. Peptide microarrays containing 185 peptides were probed with full-length and truncated pre-miRNA-155 (0.25 μM). (a) Fluorescent images of peptide microarrays incubated with miRNAs (white boxes indicate spots printed with buffer solutions as a control. (b) Quantitative analysis of fluorescence intensity of peptide microarrays probed with miRNAs. Mean fluorescence intensity was determined using five-independent experiments (mean ± SD). (c) Heatmap of 185 peptides against miRNAs. The color ruler is shown at the bottom (Fl = fluorescence intensity).

recorded (Figure S1). A comparison of peptide helicities obtained from CD spectra to their RNA binding properties arising from microarray analysis indicates that no significant correlation exists between helicities of singly substituted peptides and miRNA-155 binding affinities.

Peptide Inhibitors Suppress Dicer Catalyzed miRNA-155 Processing. Because the discovery of peptides that suppress production of oncogenic miRNA is the long-term goal of this study, the peptides selected for further investigation were evaluated for their inhibition of miRNA processing. Based on the results obtained from the microarray experiments, 12 peptides (**1**, **86**, **93**, **99**, **107**, **109**, **125**, **131**, **136**, **142**, **159**, **176**) with relatively strong binding affinities toward pre-miRNA-155 were used in an investigation designed to examine inhibition of mature miRNA-155 production catalyzed by Dicer. Peptide **26** was utilized as a control because it has a low pre-miRNA-155 binding affinity. Radioactive pre-miRNA-155 was incubated for 10 min with recombinant human Dicer in the presence of 1.5 μM of each peptide. The amount of mature miRNA-155 formed was then determined using a phosphoimager (Figures 4a and S2). Two peptides, **159** and **176**, containing Trp at the respective 11 and 12 positions, were found to significantly block miRNA-155 processing (>70% inhibition). However, other peptides with strong binding affinities to pre-miRNA-155 have no or very little inhibitory activities of Dicer-catalyzed miRNA-155 processing. These findings suggest that strong binding of peptides to pre-miRNA-155 may not be sufficient for the inhibition of Dicer-catalyzed miRNA-155 processing, but their appropriate binding to pre-miRNA-155, which leads to inhibition of Dicer activity, is important.

IC_{50} values of **159** and **176** toward inhibition of Dicer-catalyzed miRNA-155 processing were measured to be 0.77 and 1.6 μM, respectively (Figure 4b and c). Dissociation constants (K_d) for interactions between pre-miRNA-155 and **159** and **176** were determined to be 47 and 57 nM, respectively, by using peptide microarrays (Figure S3a). The K_d values were also measured by fluorescence anisotropy. Dissociation constants obtained from fluorescence anisotropy are slightly lower (26 nM for **159** and 31 nM for **176**) than those determined by using peptide microarrays (Figure S3b), but binding tendencies of two peptides to pre-miRNA-155 are similar in two methods. It should be noted that K_d values are slightly different depending on which methods are employed for measurements. It is interesting that the miRNA-155 processing inhibitory activities of Trp containing **159** and **176** correlate with the well-known increases in binding properties and biological activities of peptides caused by the introduction of Trp residues.[15,23]

On the basis of results of the peptide microarray and in vitro Dicer inhibition studies, peptides **159** (LKKLLKLLKK**W**L-KLKG) and **176** (LKKLLKLLKKL**W**KLKG) were selected for use in studies probing inhibition of Dicer-mediated miRNA-155 processing in cells. Peptide **26** (LQKLLKLLQKLLKLKG), having a weak pre-miRNA-155 binding affinity (K_d = 313 ± 71 nM, Figure S4) and a low inhibitory activity of miRNA-155

DOI: 10.1021/jacs.5b09216
J. Am. Chem. Soc. 2016, 138, 857−867

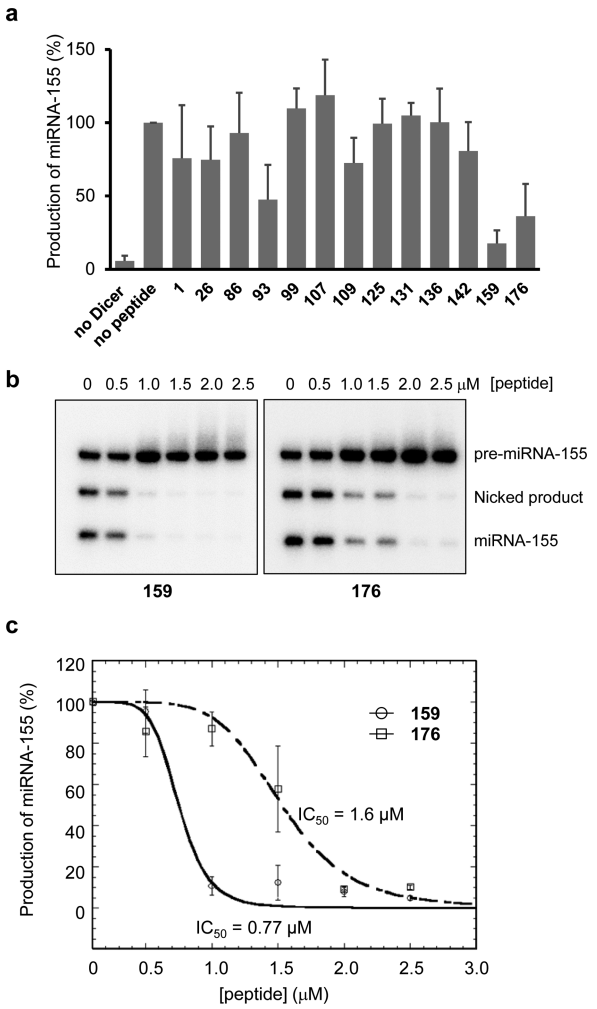

Figure 4. Effect of peptides on inhibition of miRNA-155 processing mediated by Dicer. (a) Radioactive pre-miRNA-155 was incubated with recombinant human Dicer in the presence of 1.5 μM of each peptide for 10 min. The amount of mature miRNA-155 was quantified by using a phosphoimager (mean ± SD, $n \geq 6$). (b) Representative autoradiogram of miRNA-155 processing in the presence of each peptide. Radioactive pre-miRNA-155 was incubated for 10 min with Dicer in the presence of various concentrations of **159** or **176**. (c) IC_{50} values of **159** and **176** for inhibition of miRNA-155 processing (mean ± SD, $n = 3$).

processing, was employed as a negative control. MCF-7 cells transfected with pre-miRNA-155 were treated with **159**, **176**, and **26** for 6 h.[24] The results of Northern blot analysis of the treated cells showed that **159** and **176** suppress miRNA-155 processing significantly and that the control **26** has very low inhibitory activity (Figure 5a and b), phenomena which are consistent with observations made in the in vitro experiments.

Because peptide inhibitors **159** and **176** blocked miRNA-155 processing in cells, we next determined if target genes of miRNA-155 are upregulated in cells treated with these peptides. It was reported previously that increased expression of miRNA-155 causes a substantial decrease in Forkhead box O3 (FOXO3a), which acts as a trigger for apoptosis by activating caspase-3.[25] The reduced level of FOXO3a caused by this phenomenon results in resistance of cells to apoptosis and leads to tumor growth. In addition, upregulation of miRNA-155 is also known to cause a decrease in expression of DNA mismatch repair proteins (MLH1, MSH2, MSH6), which promotes an increase in the levels of mutations that trigger cancer development.[26a] On the basis of these observations, we assessed the expression levels of FOXO3a, MLH1, MSH2 and MSH6 by using quantitative real-time PCR after MCF-7 cells were incubated with **26**, **159**, and **176** for 5 h. The results showed that expression levels of target genes increase significantly in cells treated with peptides **159** and **176**, whereas **26** causes no significant increase in expression of the genes (Figure 5c). Furthermore, four genes (suppressor of cytokine signaling 1 (SOSC1), telomeric repeat binding factor 1 (TRF-1), tumor protein p53 inducible nuclear protein 1 (TP53INP1) and adenomatous polyposis coli (APC)) whose expression is known to be suppressed by miRNA-155 are also upregulated in cells treated with peptides **159** and **176** (Figure 5c).[26b−d,27] The findings indicate that peptides **159** and **176** suppress production of mature miRNA-155 from pre-miRNA-155 and, as a consequence, induce expression of genes associated with apoptosis in cells.

We next examined if peptides **159** and **176** affect other pre-miRNA processing mediated by Dicer. Prior to this study, we determined binding affinities of four pre-miRNAs (pre-miRNA-155, pre-let7a-1, pre-miRNA-16-1, and pre-miRNA-21) and peptides **1**, **159**, and **176** by using fluorescence anisotropy or peptide microarrays. The results showed that each of peptides **1**, **159** and **176** bind to pre-miRNAs with similar binding affinities (Table S3). Then, to test the effect of peptides on Dicer catalyzed pre-miRNA processing, radioactive pre-let7a-1, pre-miRNA-16-1, and pre-miRNA-21 were incubated with Dicer for 10 min in the presence and absence of each of three peptides (1.5 μM, **1**, **159** and **176**). The amount of mature miRNAs formed was determined by using a phosphoimager. As shown in Figure S5, whereas peptide **1** has significantly low inhibitory activity of Dicer catalyzed pre-miRNA processing, **159** and **176** have good inhibitory activity. The results also revealed that **159** and **176** inhibit pre-miRNA-155 processing by Dicer more efficiently than pre-let7a-1 and pre-miRNA-21 but blocked processing of both pre-miRNA-155 and pre-miRNA-16-1 to a similar degree (Table S4).

Peptide Inhibitors Induce Caspase-Dependent Apoptosis. Because upregulation of miRNA-155 in tumors leads to resistance to apoptosis,[10,16] the peptide inhibitors should induce apoptotic cell death. To test this proposal, cell death activities of peptides were determined by incubating MCF-7 and MDA-MB-231 breast cancer cells expressing miRNA-155[27] with various concentrations (0−10 μM) of **159** and **176** as well as a control **26** for 24 h. Additionally, Ramos cells which rarely express miRNA-155[28] were also treated with each peptide under the same incubation conditions. Cell viabilities were then assessed by using an MTT (3-(4,5-dimethylthiazol-2-yl)-2,5-diphenyltetrazolium bromide) assay. The number of viable MCF-7 and MDA-MB-231 cells after treatment with **159** and **176** was found to decrease in a peptide concentration-dependent manner with half maximal inhibitory concentration (IC_{50}) values of 2−5 μM, but peptide **26** has a much lower cytotoxicity against both cell types (Figure S6). It is worthwhile mentioning that because MCF-7 cells produce more miRNA-155 than MDA-MB-231 cells,[27] MCF-7 cells are more susceptible to peptide-induced cell death than MDA-MB-231 cells. Importantly, peptides **159** and **176** have a markedly reduced activity for Ramos cell death. These findings indicate that miRNA-155 expressing cells are more susceptible to cell death promoted by the two peptides than are cells that rarely express miRNA-155.

DOI: 10.1021/jacs.5b09216
J. Am. Chem. Soc. 2016, 138, 857−867

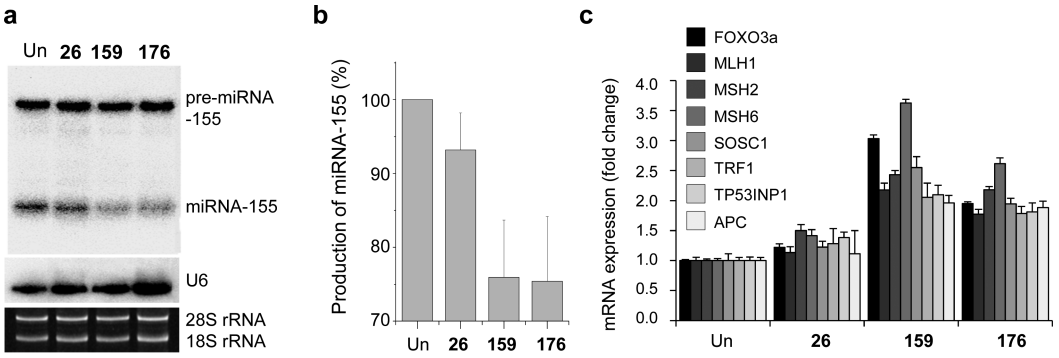

Figure 5. Effects of peptides on inhibition of miRNA-155 production in cells. (a) MCF-7 cells transfected with pre-miRNA-155 were incubated in the absence or presence of 5 μM of each peptide for 6 h. Levels of miRNA-155 were determined by using Northern blot analysis. U6 and ethidium-bromide-stained 28S and 18S rRNAs are shown as controls for equal loading. (b) Quantitative analysis of miRNA-155 production in (a) (mean ± SD, n = 3). (c) MCF-7 cells were incubated in the absence or presence of 5 μM of each peptide for 5 h. The mRNA expression of indicated genes was determined by using quantitative real-time PCR. The miRNA-155 expression was normalized to the expression of 18S rRNA (mean ± SD, n = 3).

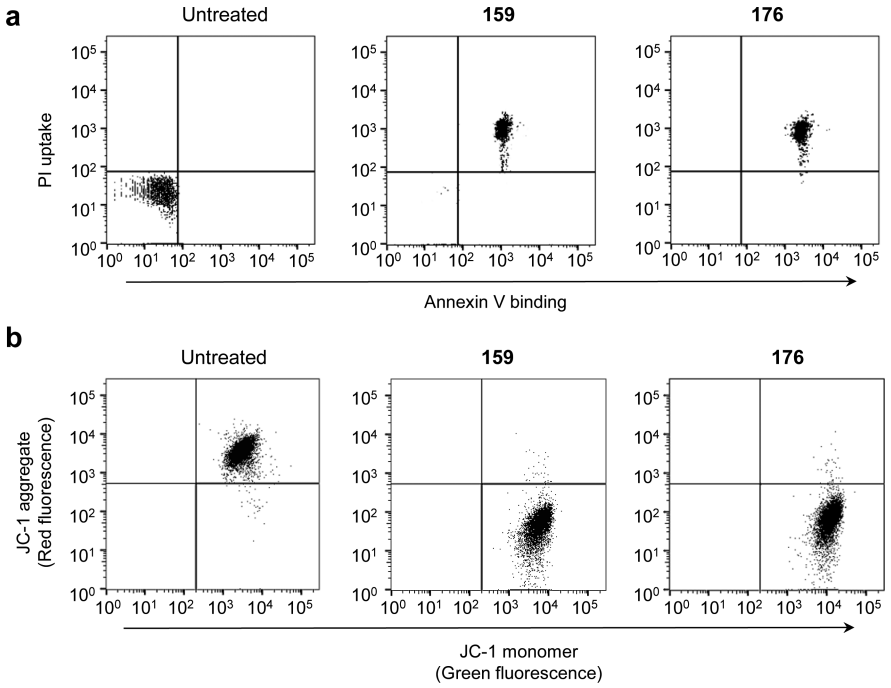

Figure 6. Peptide inhibitors induce apoptosis. (a) Flow cytometry of MCF-7 cells incubated with 10 μM of each peptide for 24 h and then stained with fluorescein-annexin V and PI. (b) Flow cytometry of MCF-7 cells incubated with 10 μM of each peptide for 24 h and then stained with JC-1. Shown is a dot plot of red fluorescence (FL2, JC-1 aggregate) versus green fluorescence (FL1, JC-1 monomer). Untreated cells were used as a negative control.

The cell permeability of peptides could affect their ability to promote cell death. To determine their cell permeability, MCF-7, MDA-MB-231 and Ramos cells were treated with N-terminal Cy5 and FITC-labeled **26**, **159**, and **176** for 4 h, and then subjected to flow cytometry analysis and confocal microscopy study. The results showed that the three peptides labeled with different dyes have similar degrees of cell permeability (Figure S7), indicating that the differences in cell death activities of the peptides are not associated with this property.

In order to evaluate whether peptide inhibitors promote cell death via apoptosis, MCF-7 cells were incubated with **159** and **176** and then treated with a mixture of fluorescein-labeled annexin V and propidium iodide (PI). The results of flow cytometry analysis revealed that both peptides induce apoptosis, as inferred from observations of positive annexin V binding and PI uptake (Figure 6a).[29] In addition, the extent of cell shrinkage, another characteristic of apoptosis, was determined. Analysis of cell size by using flow cytometry showed that peptide treated cells undergo a large degree of cell shrinkage (Figure S8). Furthermore, the loss of mitochondrial membrane potential, which is a hallmark of apoptosis, was also evaluated using a membrane potential sensitive probe JC-1.[30] The intensity of dye-derived red fluorescence in cells treated with peptide inhibitors for 24 h decreased significantly but the green fluorescence intensity was unaltered, a phenomenon which is indicative of apoptotic cell death (Figure 6b). An increase in DNA fragmentation also occurred in cells treated with the peptide inhibitors for 24 h (Figure S9). Taken together, the results provide evidence to support the conclusion

DOI: 10.1021/jacs.5b09216
J. Am. Chem. Soc. 2016, 138, 857−867

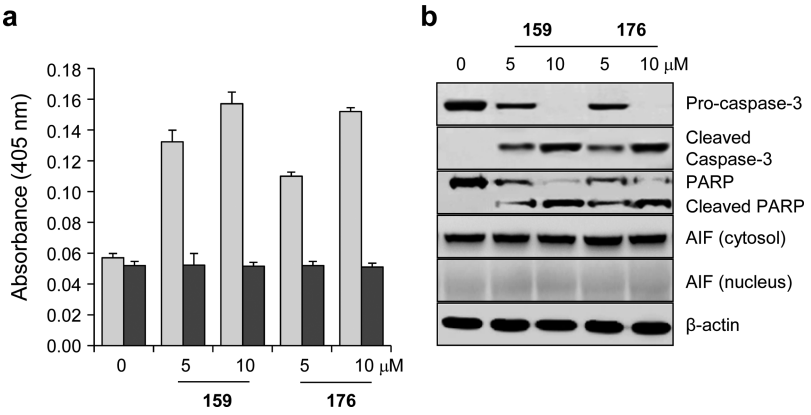

Figure 7. Peptide inhibitors induce caspase activation. (a) Caspase activities of lysates of MCF-7 cells treated with each peptide for 24 h were measured using acetyl-DEVD-pNA in the absence (gray bar) or presence (black bar) of 200 μM Ac-DEVD-CHO (mean ± SD, n = 3). (b) MCF-7 cells were treated with 10 μM of each peptide for 24 h, and the indicated proteins were immunoblotted using the appropriate corresponding antibodies.

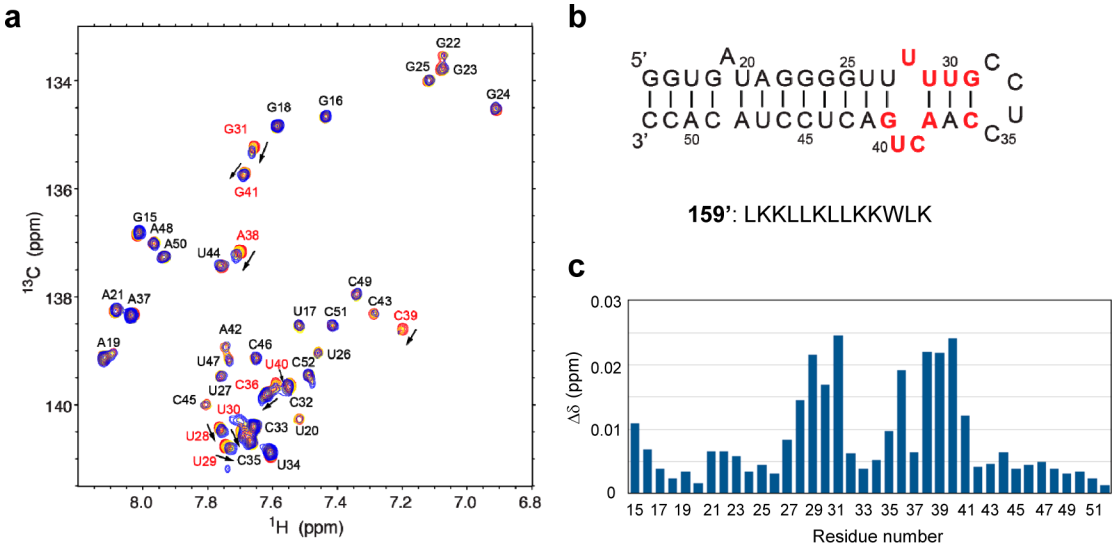

Figure 8. NMR study of binding of peptide to pre-miRNA-155. (a) Partial ^{1}H−^{13}C HSQC spectrum of truncated pre-miRNA-155 (0.1 mM) after addition of peptide **159**′ (a final concentration: red, 0; yellow, 0.05; blue, 0.1 mM). (b) Residues influenced by peptide **159**′ in NMR spectra are colored red ($\Delta\delta$ > 0.01 ppm). The sequence of peptide **159**′ is shown. (c) Chemical shift perturbations upon addition of peptide **159**′ to truncated pre-miRNA-155. The equation, $\Delta\delta$ ppm = $[(\Delta\delta\ ^{1}\text{H ppm})^2 + (\Delta\delta\ ^{13}\text{C ppm}/4)^2]^{1/2}$, was used to measure chemical shift perturbations.

that peptide inhibitors investigated in this effort promote apoptosis.

Apoptosis takes place mainly through caspase-dependent and independent pathways.[31] To determine if peptide inhibitors induce caspase-dependent apoptosis, MCF-7 cells were incubated with **159** and **176** for 24 h. The proteolytic activities associated with caspases were then measured using a colorimetric peptide substrate of caspases, Ac-DEVD-pNA (pNA, p-nitroaniline). Caspase activities were observed to increase in peptide treated cells, but almost no caspase activities were seen when Ac-DEAD-CHO, a known inhibitor of caspases, was added to peptide treated cell lysates (Figure 7a).

During the caspase-dependent apoptosis, caspase-3 is activated by the cleavage of procaspase-3.[32] The results of immunoblot analysis of the peptide treated cells showed that procaspase-3 is proteolytically cleaved to generate caspase-3 (Figure 7b). Western blot analysis also revealed that the endogenous caspase substrate, poly(ADP-ribose) polymerase (PARP), is cleaved in the peptide treated cells. These results indicate that peptide inhibitors induce apoptotic cell death via a caspase-dependent pathway.

We also examined whether the peptide inhibitors are involved in apoptosis inducing factor (AIF)-associated caspase-independent apoptosis. It is known that AIF is translocated into the nucleus during the caspase-independent apoptosis.[33] Consequently, a comparison of the AIF levels in cytosolic and nuclear fractions of cells provides a measure of apoptosis that takes place in a caspase-independent fashion. MCF-7 cells were incubated with **159** and **176** and then subjected to Western blot analysis using an AIF antibody. The results of immunoblot analysis showed that treatment with peptides does not promote translocation of AIF into the nucleus (Figure 7b). Collectively, the observations made in this study demonstrate that the peptide inhibitors identified in this study induce caspase activation but do not activate the AIF-associated caspase-independent apoptotic pathway.

Because it is known that peptide **1** binds to calmodulin and antagonists of calmodulin induce apoptotic cell death,[19,34] we investigated binding of its analogous peptides **26**, **159**, and **176**

DOI: 10.1021/jacs.5b09216
J. Am. Chem. Soc. 2016, 138, 857−867

to the protein by using fluorescence anisotropy measurements. All four peptides were found to interact with calmodulin with less than 10 nM of K_d values (Table S5). If calmodulin is one of main factors associated with cell death induced by **159** and **176**, then all peptides should have similar cell death activity. However, the results of an MTT assay show that only peptides **159** and **176** have high cytotoxicity in miRNA-155 producing cells but **1** and **26** with the similar cell permeability to **159** and **176** exhibit low cell death activity (Figures S6 and S7). These results suggest that calmodulin may not be a main target of **159** and **176** to induce apoptotic cell death.

NMR Studies. To gain information about the mode of binding of the peptide inhibitors to pre-miRNA-155, we first determined the secondary structure of pre-miRNA-155 by using 2D ^{1}H−^{1}H NOESY NMR spectroscopy. Because truncated pre-miRNA-155 (U17-A50, Figure 2c) was found to interact with peptides in patterns that are similar to that of full-length pre-miRNA-155 (Figure 3), the truncated RNA was used for these structural studies. Watson−Crick base pairs of RNA were identified utilizing NOEs between imino and imino, imino and aromatic, and imino and amino protons in 2D spectra (Figure S10). Apical stem-loop base pairs (U29-A38, U30-A37, and G31-C36) were assigned based on NOEs for imino protons of U30 and G31. This base pair assignment was further supported by NOEs for A38H2−U30H1′ and A37H2−G31H1′, types of cross-strand NOEs that are normally observed for base-paired regions of A-form helical RNA structures.[35] The bugle nucleotide A19 appears to be stacked between the bases G18 and U20, because standard H1′-base sequential connectivity from G18 to U20 and the cross-strand NOE for A19H2−C49H1′ were observed in the spectra. In addition, analysis of 2D NOSEY spectra also indicates that G-U wobble base pairs (G24-U44 and U27-G41) are present.[36] The secondary structure of pre-miRNA-155, assigned by utilizing this NMR analysis, is shown in Figure S10.

Next, chemical shift perturbations of resonances for carbons and protons of RNA bases were evaluated in order to gain information about regions of pre-miRNA-155 that are responsible for interactions with peptides.[37,38] Peptide **159**′ (LKKLLKLLKK**W**LK), in which three amino acids at the C-terminus of **159** that are seldom involved in RNA binding were deleted, was employed for this purpose. Chemical shift changes induced by addition of 0 to 1 equiv of **159**′ to truncated pre-miRNA-155 were determined by using 2D ^{1}H−^{13}C HSQC spectroscopy (Figure 8). Most carbon and proton resonances in the RNA bases were found to undergo very small chemical shift changes ($\Delta\delta_{max}$ < 0.03) upon addition of **159**′. This observation indicates that binding of peptide **159**′ to the RNA does not induce any large RNA conformational change. Importantly, relatively large chemical shift perturbations ($\Delta\delta_{max}$ > 0.01 ppm) were observed in bases U28−G31, C36 and A38−G41. This finding suggests that peptide **159**′ preferentially binds to the upper bulge and apical stem-loop region of pre-miRNA-155.

We showed that peptide **1** has a similar binding affinity to pre-miRNA-155 (Table S3) but lower inhibitory activity toward miRNA-155 processing catalyzed by Dicer in comparison to peptide **159** (Figure S2). In order to address the distinctive bioactivity between **159** and **1**, we also performed NMR chemical shift perturbation experiments with truncated pre-miRNA-155 and **1**′ (LKKLLKLLKKLLK) with deletion of three amino acids at the C-terminus of **1**. The NMR data analysis showed the different levels of chemical shift perturbations of resonances for pre-miRNA-155 bases, particularly U29, U30, C36, and A42, when **1**′ and **159**′ are added to a solution of RNA (Figure S11). This finding suggests that the local binding interface between **159**′ and pre-miRNA-155 are different from that between **1**′ and pre-miRNA-155. Because the structures of pre-miRNA-155 as well as its complex with Dicer have not been determined yet, we surmise that slightly different pre-miRNA-155 conformations upon binding to the two peptides may reflect their distinctive bioactivities toward miRNA-155 processing catalyzed by Dicer.

Molecular Modeling Studies. To gain insight into the binding mode of inhibitor **159** to pre-miRNA-155, molecular modeling studies of a complex of truncated pre-miRNA-155 with **159** were performed by using the MC-Sym method.[37] Experimentally determined NMR constraints, arising from analyses of chemical shifts and chemical shift perturbations, were utilized to build the model. Analysis of the model of the complex suggests that both hydrophilic and hydrophobic side chains of amino acids 4−12 in **159** are mostly involved in binding to pre-miRNA-155 bases or phosphate groups through electrostatic, hydrogen bonding and van der Waals interactions. The results of molecular modeling study also suggest that binding of **159** to the major groove of the apical stem-loop region of pre-miRNA-155 may cause suppression of the cleavage of pre-miRNA-155 catalyzed by Dicer (Figure 9).

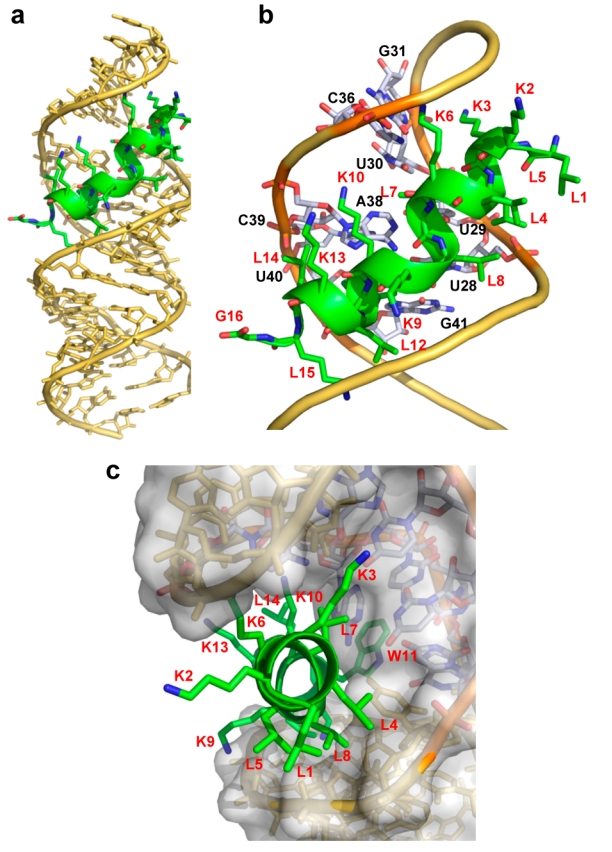

Figure 9. Molecular models of a complex of peptide **159** with truncated pre-miRNA-155. (a) Overall structure of pre-miRNA-155 (yellow) complexed with peptide **159** (green). Side chains of peptide are located within the major groove of the apical stem-loop region of pre-miRNA-155. (b) Close side-view of the complex (peptide residue number; red, RNA base number; black). (c) Top-view of the solvent-accessible surface of the major groove of RNA complexed with **159**.

DOI: 10.1021/jacs.5b09216
J. Am. Chem. Soc. 2016, 138, 857−867

CONCLUSION

MiRNA-155 is one of the most potent miRNAs that suppress apoptosis in cancer cells. Thus, inhibitors of Dicer catalyzed miRNA-155 processing can be used as chemical probes in studies targeted at gaining an understanding of the biological role of miRNA-155 as well as lead substances in efforts aimed at developing new therapeutic agents for cancer treatment. In the investigation described above, peptide microarrays were employed for rapid analysis of binding of 185 peptides to pre-miRNA-155. The results suggest that both the position and nature of the amino acid mutations significantly affect binding affinities of peptides to pre-miRNA-155. The results of in vitro Dicer inhibition studies showed that two tight binding peptides in this group suppress miRNA-155 processing and, as a result, enhance expression of miRNA-155 target genes in cells. We also found that the selected two peptides block in vitro pre-miRNA-155 processing catalyzed by Dicer more efficiently than pre-let7a-1 and pre-miRNA-21 but similarly inhibit processing of both pre-miRNA-155 and pre-miRNA-16-1. The two peptides blocking miRNA-155 processing may serve as promising leads to further identify more selective molecules to inhibit miRNA-155 processing.

Cell study provides evidence to support the conclusion that the two peptides promote apoptotic cell death via a caspase-dependent pathway. Finally, observations made in NMR and molecular modeling studies suggest that the peptide inhibitors mainly bind to the apical stem-loop region of pre-miRNA-155, thereby blocking Dicer-catalyzed miRNA-155 processing. The results of this effort clearly demonstrate the merits of using peptide microarrays to identify ligands that target miRNAs in a rapid manner.

EXPERIMENTAL SECTION

Full details of all experimental procedure not presented below are provided in the Supporting Information.

Preparation of Peptide Microarrays. The hydrazide-conjugated peptides dissolved in 100 mM sodium phosphate buffer (pH 5.4) containing 40% glycerol were placed into the wells of a 384-well plate. Each peptide (1 nL) was printed in duplicate at predetermined places on an epoxide-derivatized glass slide,[20,21] with a distance of 270 μm between the centers of adjacent spots by using a pin-type microarrayer (MicroSys 5100 PA, Cartesian Technologies). After completion of printing, the slide was placed into a humid chamber (55−60% relative humidity) at room temperature for 5 h. The slide was then divided into several blocks by using a compartmentalized plastic film that was coated with adhesive on one side (thickness: 0.1−0.2 mm) to avoid cross-contamination. The slide was washed three times with PBS buffer (pH 7.4) containing 0.1% Tween-20 under gentle shaking for 5 min. After drying the slide by purging with argon gas, a solution (15−20 μL) of 10 mM $NaHCO_3$ (pH 8.3) containing 1% 2-aminoethanol was dropped onto the compartmented block and then left at room temperature for 0.5 h. The slide was washed 3 times with PBS buffer (pH 7.4) containing 0.1% Tween-20 under gentle shaking for 5 min. To obtain reproducible results, the prepared peptide microarrays were used immediately.

Evaluation of Interactions of Pre-miRNA-155 with Peptides Using Peptide Microarrays. Solutions (15−20 μL) of 0.25 μM of full-length or truncated pre-miRNA-155 (Dharmacon) labeled by Dye 547 in 20 mM HEPES (pH 7.4) containing 1 mM $MgCl_2$, 5 mM KCl, 140 mM NaCl, and 0.05% Tween-20 were dropped onto each block of peptide microarrays and then incubated for 1 h at room temperature. Unbound pre-miRNA-155 was removed by washing the slide with PBS buffer containing 0.1% Tween-20 (3 min ×3). After washing by purging with argon gas, the slide was scanned using an ArrayWoRx biochip reader (Applied Precision).

NMR Study. Unlabeled, uniformly and base-specifically (AU and GC) $^{13}C,^{15}N$-labeled, truncated pre-miRNA-155 was prepared by using in vitro transcription with His_6-tagged P266L bacteriophage T7 polymerase mutant 1 with synthetic DNA templates (Integrated DNA Technologies). The synthesized RNAs were precipitated with ethanol, purified using 15% denaturing PAGE, electroeluted (Elutrap, Whatman), and subjected to an anion-exchange column (GE healthcare). Fractions containing the purified RNAs were dialyzed against water by using an Amicon filtration system (Millipore). The dilute solutions (ca. 10 μM) of the RNA were heated to 95 °C, cooled on ice, and concentrated to 1−1.5 mM. NMR samples were prepared in 10 mM sodium phosphate buffer (pH 7.4) with 10% D_2O for assignments of exchangeable protons, and 100% D_2O for assignments of non-exchangeable protons. To identify peptide-binding residues of pre-miRNA-155, **159′** (LKKLLKLLKKWLK) or **1′** (LKKLLKLLKKLLK) was added to 0.1 mM pre-miRNA-155 in 10 mM sodium phosphate buffer (pH 7.4) with 5% DMSO-d_6 and 10% D_2O (a final concentration of peptide: 0, 0.05, and 0.1 mM).

NMR spectra were recorded using an Agilent DD2 600 MHz instrument with a *z*-gradient triple resonance probe and Bruker 800 and 900 MHz spectrometers equipped with *z*-shielded gradient triple resonance cryoprobes at 10 °C for exchangeable and 20 °C for nonexchangeable proton spectra. The imino-exchangeable protons were assigned by analysis of 2D NOESY and 2D $^1H-^{15}N$ HSQC spectra. Ribose H1′ protons and base H2/H5/H6/H8 protons were sequentially assigned from analyses of 2D NOESY and 2D TOCSY spectra of unlabeled RNA samples. For unambiguous assignments of nuclei resonating in overlapped regions, 2D $^1H-^{13}C$ HSQC and 2D-filtered/edited NOESY (F2f and F1fF2f) spectra were recorded with base type-specific $^{13}C,^{15}N$-labeled RNA. The base C2/C6/C8 carbons were assigned from the analysis of 2D NOESY and 2D $^1H-^{13}C$ HSQC spectra. The 2D $^1H-^{13}C$ HSQC spectra were analyzed to monitor chemical shift changes upon addition of the peptide to RNA. NMR spectra were processed and analyzed using topspin 3.1 (Bruker) and Sparky 3.115 (University of California, San Francisco, CA).

Molecular Modeling Study. A total of 418 3-D models of truncated pre-miRNA-155 were generated using MC-Sym 4.2, followed by GB/SA (generalized Born surface area) energy minimization using Amber tools. An α-helix model of peptide **159** was generated by using Discovery Studio 4.1 (BIOVIA) and docked with the modeled pre-miRNA-155 structures with only translation and rotational freedom (rigid-body docking) using rDock. A structural model was selected based on the lowest weighted mean absolute errors (wMAE) between measured and predicted ^1H and ^{13}C chemical shifts (total 188 resonance assignments) of each RNA model structure followed by 1 ns molecular dynamics simulation in a box of explicit water molecules using GROMACS 4. Model structures are viewed in Pymol (Schrodinger, LLC).

Effect of Peptides on miRNA-155 Production in Cells. MCF cells at 60−70% confluency in 6-well plates were transfected with pre-miRNA155 using Dharmafect I (GE Healthcare Life Sciences) according to the manufacture's protocol. Per well, 10 pmol of pre-miRNA-155 and 1 μg of Dharmafect I were used. The cells were transfected in Opti-MEM (Life Technologies) media for 24 h and treated with peptides in fresh complete media for 6 h.

Northern blot assays were performed in the manner as described previously.[15] Briefly, RNAs isolated from MCF-7 cells using TRIzol (Life Technologies) were resolved on 12.5% denaturing polyacrylamide gel with 7 M urea. RNAs were transferred to a neutral nylon membrane (Hybond NX, GE Healthcare Life Sciences). Blotting was carried out with the 5′-radioactively [γ-^{32}P] labeled DNA oligo probes:

miRNA-155: 5′-ACCCCTATCACGATTAGCATTAA-3′

U6 snRNA: 5′-TAGTATATGTGCTGCCGAAGCGAGCA-3′

Quantitative Real-Time PCR. Total RNAs were extracted with TRIzol using the protocol provided by the manufacturer. One microgram of RNA was reverse transcribed with Superscripts III (Life Technologies) using OligodT primer and RNA was removed using RNase H (NEB). Quantitative real time-PCR was performed on a CFX96 (Bio-Rad). cDNA template 2 μL (100 ng), 0.4 μL (10 μM) of forward and reverse primers (see below), and 10 μL of Sybr Premix Ex

DOI: 10.1021/jacs.5b09216
J. Am. Chem. Soc. 2016, 138, 857−867

Taq (TaKaRa, Japan) in a total volume of 20 μL were applied to the following PCR programs: 30 s 95 °C (initial denaturation); 20 °C/s temperature transition rate up to 95 °C for 10 s, 30 s, 60 °C, 10 s 72 °C, repeated 40 times (amplification). 18S was used for normalization. The primers used for this study are listed in Table S2.

Measurement of Cell Death. MCF-7, MDA-MB-231, and Ramos cells were cultured in RPMI 1640 (Invitrogen) supplemented with 10% fetal bovine serum (FBS), 50 units/mL penicillin, and 50 units/mL streptomycin, and maintained at 37 °C under a humidified atmosphere of 5% CO_2. The cells (5×10^3 in 96-well plate) were incubated with various concentrations of each peptide in culture media. MTT assays were performed using standard procedures. The absorbance at 570 nm was measured using an Infinite 200 PRO multimode microplate reader (TECAN, Austria).

Flow Cytometry. MCF-7 cells were treated with 10 μM of each peptide for 24 h. Untreated cells were used as a negative control. After washing with PBS twice, the cells were incubated with 0.5 mL of trypsin-EDTA (0.05% trypsin, 0.02% EDTA, Sigma-Aldrich) for 5−10 min at 37 °C and collected. Cells were resuspended in binding buffer (500 μL, 10 mM HEPES/NaOH, pH 7.5 containing 1.4 M NaCl and 2.5 mM $CaCl_2$) and treated with a mixture of fluorescein-annexin V (final concentration = 0.5 μg/mL) and propidium iodide (final concentration = 2 μg/mL) for 10 min at room temperature. For JC-1 staining, cells were resuspended using PBS containing JC-1 (final concentration = 2.5 μg/mL, Anaspec), incubated for 15 min, and washed with PBS twice. Flow cytometry was performed using a BD FACSVerse instrument (BD Biosciences) and a FlowJo software (BD Biosciences). The intensity of the red fluorescence signal was measured using an excitation wavelength of 550 nm and an emission wavelength of 600 nm. The intensity of the green fluorescence was measure using an excitation wavelength of 485 nm and monitoring the emission at 535 nm.

Caspase Activity Assay. MCF-7 cells were incubated with 0, 5, and 10 μM of each peptide for 24 h. The cells were lysed in a buffer containing 50 mM HEPES, pH 7.4, 5 mM CHAPS, 5 mM DTT. Cell lysates were placed into the appropriate wells of a 96-well plate. Assay buffer containing 20 mM HEPES, pH 7.4, 0.01% CHAPS, 5 mM DTT, and 2 mM EDTA was added to each well. The caspase inhibitor Ac-DEVD-CHO (20 μM) was added to the wells. Caspase activity was determined by adding acetyl-DEVD-pNA (200 μM) (Sigma-Aldrich) to the wells. The enzyme-catalyzed release of pNA was monitored at 405 nm using an Infinite 200 PRO multimode microplate reader (TECAN).

Western Blot Analysis. Proteins were separated by 6−12% SDS-PAGE. Mouse procaspase-3 monoclonal (1:1000, Santa Cruz Bio Technology), rabbit cleaved caspase-3 polyclonal (1:1000, Santa Cruz Bio Technology), rabbit PARP polyclonal (1:1000, Cell Signaling Technology), rabbit AIF polyclonal (1:1000, Santa Cruz Bio Technology), and mouse β-actin (1:1000, Santa Cruz Bio Technology) antibodies were used as primary antibodies. Horse peroxidase-conjugated goat anti-rabbit IgG (1:2000, Santa Cruz Bio Technology) and goat anti-mouse IgG (1:2000, Santa Cruz Bio Technology) were used as secondary antibodies. The blots were developed using an West-ZOL plus Western Blot Detection System (Intron Biotechnology Inc., South Korea). The Western blot signal was then analyzed by using a G:BOX Chemi Fluorescent & Chemiluminescent Imaging System (Syngene).

■ ASSOCIATED CONTENT

Supporting Information

The Supporting Information is available free of charge on the ACS Publications website at DOI: 10.1021/jacs.5b09216.

Additional experimental procedure details; sequences and MS data of synthesized peptides; primers used for quantitative real-time PCR; K_A values for interaction between peptides and pre-miRNAs, and between peptides and calmodulin; relative Dicer processing ratios of pre-miRNAs; CD spectra; autoradiograms; cytotoxicity of peptides in tested cell lines; cell permeability of peptides; DNA fragmentation in cells treated with peptide inhibitors; 2D $^1H-^1H$ NOESY and NMR data (PDF)

■ AUTHOR INFORMATION

Corresponding Authors

*injae@yonsei.ac.kr
*jhoonyu@snu.ac.kr
*nkkim@kist.re.kr

Notes

The authors declare no competing financial interest.

■ ACKNOWLEDGMENTS

This study was supported financially by the National Creative Research Initiative (2010-0018272 to I.S.) and NRL (2011-0028483 to J.Y) programs, KIST (2 V04081 and 2E25570 to N.-K.K) and NRF (2015R1A2A2A04005596 to N.-K.K) in Korea.

■ REFERENCES

(1) Bartel, D. P. *Cell* **2004**, *116*, 281−297.
(2) Cullen, B. R. *Mol. Cell* **2004**, *16*, 861−865.
(3) (a) Lee, Y.; Ahn, C.; Han, J. J.; Choi, H.; Kim, J.; Yim, J.; Lee, J.; Provost, P.; Rådmark, O.; Kim, S.; Kim, V. N. *Nature* **2003**, *425*, 415−419. (b) Denli, A. M.; Tops, B. B. J.; Plasterk, R. H.; Ketting, R. F.; Hannon, G. J. *Nature* **2004**, *432*, 231−235. (c) Gregory, R. I.; Yan, K. P.; Amuthan, G.; Chendrimada, T.; Doratotaj, B.; Cooch, N.; Shiekhattar, R. *Nature* **2004**, *432*, 235−240.
(4) (a) Bernstein, E.; Caudy, A. A.; Hammond, S. M.; Hannon, G. J. *Nature* **2001**, *409*, 363−366. (b) Ketting, R. F.; Fischer, S. E. J.; Bernstein, E.; Sijen, T.; Hannon, G. J.; Plasterk, R. H. A. *Genes Dev.* **2001**, *15*, 2654−2659.
(5) (a) Yi, R.; Qin, Y.; Macara, I. G.; Cullen, B. R. *Genes Dev.* **2003**, *17*, 3011−3016. (b) Grishok, A.; Pasquinelli, A. E.; Conte, D.; Li, N.; Parrish, S.; Ha, I.; Baillie, D. L.; Fire, A.; Ruvkun, G.; Mello, C. C. *Cell* **2001**, *106*, 23−34.
(6) (a) Diederichs, S.; Haber, D. A. *Cell* **2007**, *131*, 1097−1108. (b) Rana, T. M. *Nat. Rev. Mol. Cell Biol.* **2007**, *8*, 23−36.
(7) Filipowicz, W.; Bhattacharyya, S. N.; Sonenberg, N. *Nat. Rev. Genet.* **2008**, *9*, 102−114.
(8) (a) Lu, J.; Getz, G.; Miska, E. A.; Alvarez-Saavedra, E.; Lamb, J.; Peck, D.; Sweet-Cordero, A.; Ebert, B. L.; Mak, R. H.; Ferrando, A. A.; Downing, J. R.; Jacks, T.; Horvitz, H. R.; Golub, T. R. *Nature* **2005**, *435*, 834−838. (b) He, L.; Thomson, J. M.; Hemann, M. T.; Hernando-Monge, E.; Mu, D.; Goodson, S.; Powers, S.; Cordon-Cardo, C.; Lowe, S. W.; Hannon, G. J.; Hammond, S. M. *Nature* **2005**, *435*, 828−833.
(9) Wahlquist, C.; Jeong, D.; Rojas-Muñoz, A.; Kho, C.; Lee, A.; Mitsuyama, S.; van Mil, A.; Park, W. J.; Sluijter, J. P.; Doevendans, P. A.; Hajjar, R. J.; Mercola, M. *Nature* **2014**, *508*, 531−535.
(10) (a) Li, J.; Tan, S.; Kooger, R.; Zhang, C.; Zhang, Y. *Chem. Soc. Rev.* **2014**, *43*, 506−517. (b) Velagapudi, S. P.; Gallo, S. M.; Disney, M. D. *Nat. Chem. Biol.* **2014**, *10*, 291−297. (c) Gumireddy, K.; Young, D. D.; Xiong, X.; Hogenesch, J. B.; Huang, Q.; Deiters, A. *Angew. Chem., Int. Ed.* **2008**, *47*, 7482−7484. (d) Young, D. D.; Connelly, C. M.; Grohmann, C.; Deiters, A. *J. Am. Chem. Soc.* **2010**, *132*, 7976−7981. (e) Thomas, J. R.; Hergenrother, P. J. *Chem. Rev.* **2008**, *108*, 1171−1224.
(11) Leeper, T. C.; Athanassiou, Z.; Dias, R. L. A.; Robinson, J. A.; Varani, G. *Biochemistry* **2005**, *44*, 12362−12372.
(12) (a) Das, C.; Frankel, A. D. *Biopolymers* **2003**, *70*, 80−85. (b) Heaphy, S.; Dingwall, C.; Ernberg, I.; Gait, M. J.; Green, S. M.; Karn, J.; Lowe, A. D.; Singh, M.; Skinner, M. A. *Cell* **1990**, *60*, 685−693. (c) Zhou, Q.; Sharp, P. A. *Science* **1996**, *274*, 605−610. (d) Lee,

DOI: 10.1021/jacs.5b09216
J. Am. Chem. Soc. 2016, 138, 857−867

Y.; Hyun, S.; Kim, H. J.; Yu, J. *Angew. Chem., Int. Ed.* **2008**, *47*, 134−137.
(13) Pai, J.; Yoon, T.; Kim, N. D.; Lee, I. S.; Yu, J.; Shin, I. *J. Am. Chem. Soc.* **2012**, *134*, 19287−19296.
(14) Jang, S.; Hyun, S.; Kim, S.; Lee, S.; Lee, I. S.; Baba, M.; Lee, Y.; Yu, J. *Angew. Chem., Int. Ed.* **2014**, *53*, 10086−10089.
(15) Hyun, S.; Han, A.; Jo, M. H.; Hohng, S.; Yu, J. *ChemBioChem* **2014**, *15*, 1651−1659.
(16) Esquela-Kerscher, A.; Slack, F. J. *Nat. Rev. Cancer* **2006**, *6*, 259−269.
(17) (a) Fabani, M. M.; Abreu-Goodger, C.; Williams, D.; Lyons, P. A.; Torres, A. G.; Smith, K. G.; Enright, A. J.; Gait, M. J.; Vigorito, E. *Nucleic Acids Res.* **2010**, *38*, 4466−4475. (b) Babar, I. A.; Cheng, C. J.; Booth, C. J.; Liang, X.; Weidhaas, J. B.; Saltzman, W. M.; Slack, F. J. *Proc. Natl. Acad. Sci. U. S. A.* **2012**, *109*, E1695−E1704.
(18) (a) Stiffler, M. A.; Chen, J. R.; Grantcharova, V. P.; Lei, Y.; Fuchs, D.; Allen, J. E.; Zaslavskaia, L. A.; MacBeath, G. *Science* **2007**, *317*, 364−369. (b) Tomizaki, K. Y.; Usui, K.; Mihara, H. *ChemBioChem* **2005**, *6*, 782−799. (c) Salisbury, C. M.; Maly, D. J.; Ellman, J. A. *J. Am. Chem. Soc.* **2002**, *124*, 14868−14870. (d) Su, J.; Bringer, M. R.; Ismagilov, R. F.; Mrksich, M. *J. Am. Chem. Soc.* **2005**, *127*, 7280−7281. (e) Schutkowski, M.; Reimer, U.; Panse, S.; Dong, L. Y.; Lizcano, J. M.; Alessi, D. R.; Schneider-Mergener, J. *Angew. Chem., Int. Ed.* **2004**, *43*, 2671−2674. (f) Kohn, M.; Gutierrez-Rodriguez, M.; Jonkheijm, P.; Wetzel, S.; Wacker, R.; Schroeder, H.; Prinz, H.; Niemeyer, C. M.; Breinbauer, R.; Szedlacsek, S. E.; Waldmann, H. *Angew. Chem., Int. Ed.* **2007**, *46*, 7700−7703. (g) Uttamchandani, M.; Wang, J.; Li, J.; Hu, M.; Sun, H.; Chen, K. Y.-T.; Liu, K.; Yao, S. Q. *J. Am. Chem. Soc.* **2007**, *129*, 7848−7858. (h) Tian, X.; Pai, J.; Shin, I. *Chem. - Asian J.* **2012**, *7*, 2052−2060.
(19) Cox, J. A.; Comte, M.; Fitton, J. E.; DeGrado, W. F. *J. Biol. Chem.* **1985**, *260*, 2527−2534.
(20) Lee, M. R.; Shin, I. *Angew. Chem., Int. Ed.* **2005**, *44*, 2881−2884.
(21) (a) Park, S.; Shin, I. *Org. Lett.* **2007**, *9*, 1675−1678. (b) Park, S.; Lee, M. R.; Shin, I. *Nat. Protoc.* **2007**, *2*, 2747−2758.
(22) (a) Dertinger, D.; Uhlenbeck, O. C. *RNA* **2001**, *7*, 622−631. (b) García-García, C.; Draper, D. E. *J. Mol. Biol.* **2003**, *331*, 75−88.
(23) Lee, S. J.; Hyun, S.; Kieft, J. S.; Yu, J. *J. Am. Chem. Soc.* **2009**, *131*, 2224−2230.
(24) Schmittgen, T. D.; Lee, E. J.; Jiang, J. M.; Sarkar, A.; Yang, L. Q.; Elton, T. S.; Chen, C. F. *Methods* **2008**, *44*, 31−38.
(25) Kong, W.; He, L.; Coppola, M.; Guo, J.; Esposito, N. N.; Coppola, D.; Cheng, J. Q. *J. Biol. Chem.* **2010**, *285*, 17869−17879.
(26) (a) Valeri, N.; Gasparini, P.; Fabbri, M.; Braconi, C.; Veronese, A.; Lovat, F.; Adair, B.; Vannini, I.; Fanini, F.; Bottoni, A.; Costinean, S.; Sandhu, S. K.; Nuovo, G. J.; Alder, H.; Gafa, R.; Calore, F.; Ferracin, M.; Lanza, G.; Volinia, S.; Negrini, M.; McIlhatton, M. A.; Amadori, D.; Fishel, R.; Croce, C. M. *Proc. Natl. Acad. Sci. U. S. A.* **2010**, *107*, 6982−6987. (b) Jiang, S.; Zhang, H.-W.; Lu, M.-H.; He, X.-H.; Li, Y.; Gu, H.; Liu, M.-F.; Wang, E.-D. *Cancer Res.* **2010**, *70*, 3119−3127. (c) Dinami, R.; Ercolani, C.; Petti, E.; Piazza, S.; Ciani, Y.; Sestito, R.; Sacconi, A.; Biagioni, F.; le Sage, C.; Agami, R.; Benetti, R.; Mottolese, M.; Schneider, C.; Blandino, G.; Schoeftner, S. *Cancer Res.* **2014**, *74*, 4145−4156. (d) Lu, Y.; Xiao, J.; Lin, H.; Bai, Y.; Luo, X.; Wang, Z.; Yang, B. *Nucleic Acids Res.* **2009**, *37*, e24.
(27) Zhang, C. M.; Zhao, J.; Deng, H. Y. *Mol. Cell. Biochem.* **2013**, *379*, 201−211.
(28) Kluiver, J.; Van den Berg, A.; de Jong, D.; Blokzijl, T.; Harms, G.; Bouwman, E.; Jacobs, S.; Poppema, S.; Kroesen, B. J. *Oncogene* **2007**, *26*, 3769−3776.
(29) (a) Williams, D. R.; Ko, S.-K.; Park, S.; Lee, M.-R.; Shin, I. *Angew. Chem., Int. Ed.* **2008**, *47*, 7466−7469. (b) Ko, S. -K; Kim, J.; Na, D. C.; Park, S.; Park, S.-H.; Hyun, J. Y.; Baek, K.-H.; Kim, N. D.; Kim, N. − K.; Park, Y. N.; Song, K.; Shin, I. *Chem. Biol.* **2015**, *22*, 391−403.
(30) Ko, S.-K.; Kim, S. K.; Share, A.; Lynch, V. M.; Park, J.; Namkung, W.; Van Rossom, W.; Busschaert, N.; Gale, P. A.; Sessler, J. L.; Shin, I. *Nat. Chem.* **2014**, *6*, 885−892.
(31) Elmore, S. *Toxicol. Pathol.* **2007**, *35*, 495−516.
(32) Li, P.; Nijhawan, D.; Budihardjo, I.; Srinivasula, S. M.; Ahmad, M.; Alnemri, E. S.; Wang, X. *Cell* **1997**, *91*, 479−489.
(33) Joza, N.; Susin, S. A.; Daugas, E.; Stanford, W. L.; Cho, S. K.; Li, C. Y.; Sasaki, T.; Elia, A. J.; Cheng, H. Y.; Ravagnan, L.; Ferri, K. F.; Zamzami, N.; Wakeham, A.; Hakem, R.; Yoshida, H.; Kong, Y. Y.; Mak, T. W.; Zúñiga-Pflücker, J. C.; Kroemer, G.; Penninger, J. M. *Nature* **2001**, *410*, 549−554.
(34) Chen, Y.; Pawar, P.; Pan, G.; Ma, L.; Liu, H.; McDonald, J. M. *J. Cell. Biochem.* **2008**, *103*, 788−799.
(35) Scott, L. G.; Hennig, M. *Methods Mol. Biol.* **2008**, *452*, 29−61.
(36) Varani, G.; McClain, W. H. *EMBO Rep.* **2000**, *1*, 18−23.
(37) Williamson, M. P. *Prog. Nucl. Magn. Reson. Spectrosc.* **2013**, *73*, 1−16.
(38) Parisien, M.; Major, F. *Nature* **2008**, *452*, 51−55.

DOI: 10.1021/jacs.5b09216
J. Am. Chem. Soc. 2016, 138, 857−867